Mesoanalysis of the Interactions of Precipitating Convection and the Boundary Layer

Ruiyu Sun, Steven K. Krueger, Yaping Li, and Michael A. Zulauf, University of Utah, Salt Lake City, UT

Introduction

The boundary layer wind and thermodynamic fields contain a great deal of information about convective cloud systems (see Figures 1 and 2).The existing observational systems at the ARM Southern Great Plains (SGP) Atmospheric Climate Research Facility (ACRF) can be used to provide an extensive statistical characterization of updrafts and downdrafts in convective cloud systems. We are producing several datasets that should be useful for quantifying the characteristics of precipitating convection over land and the effects of the convection on the boundary layer. Such datasets can be used for many purposes, including evaluating cumulus parameterizations in global and mesoscale models, and for evaluating cloud-system resolving models.

This poster shows our preliminary results about how to estimate the mesonet-averaged cloud-base updraft and downdraft mass fluxes from the surface divergence field and the evaluation of this method using a 3D CRM simulation of maritime tropic convective cloud systems observed during KWAJEX and a 2D CRM simulation of convective systems observed during ARM July 1997 IOP.

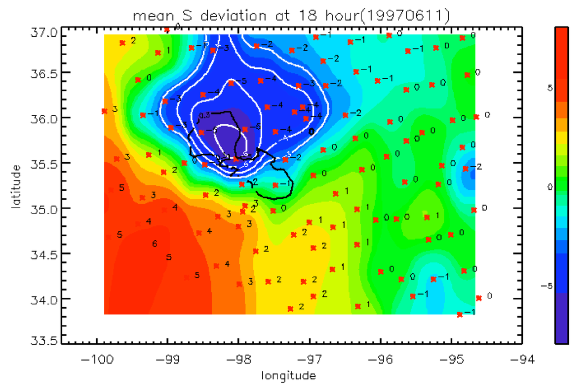

Figure 1. Deviation of static energy ($s = c_pT+gz$) from mesonet mean (location of cold pool) overlaid with gridded hourly precipitation amount contours.

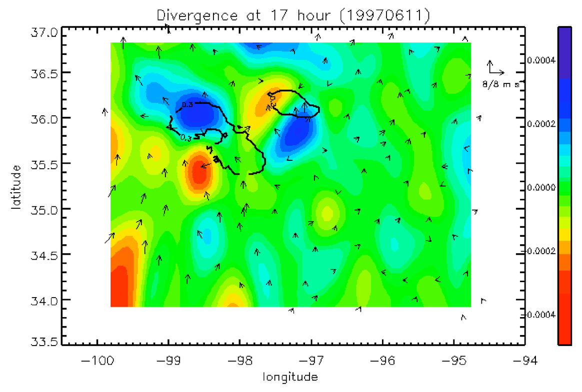

Figure 2. Divergence overlaid with gridded hourly precipitation amount.

Data Sources

We are using two observational datasets. One contains hourly accumulated precipitation amounts gridded in the HRAP coordinates system with a grid size of approximately 4 km. The second is the Oklahoma Mesonet surface data. It includes standard surface meteorological measurements that are averaged over 5-minute intervals. At this time, we are analyzing two time periods: May-August 1997 and 2000. The averaged distance between stations is about 40 km.

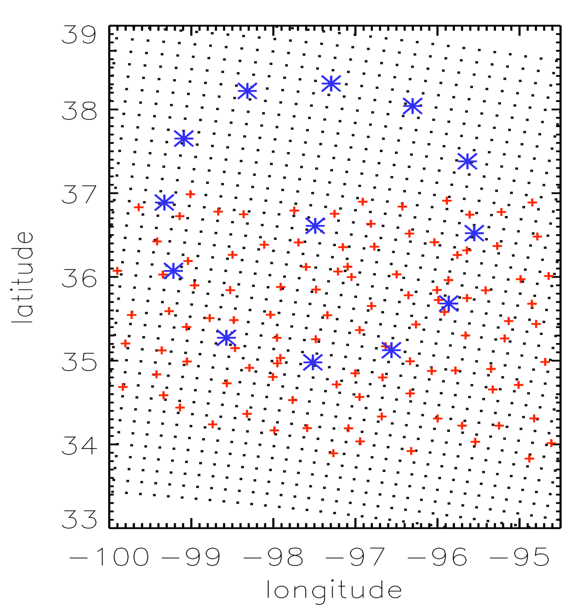

Figure 3. The analysis domain. Grid points of gridded hourly precipitation amount data (dots), locations of Oklahoma Mesonet stations(red +), and SGP SCM domain (blue stars)

Method of Analysis and Preliminary Results

Divergence Calculation

In Figures 2 and 3, each triangle is colored according to its divergence value. We define M_u and M_d, where div_i is the horizontal divergence of the ith triangle, which has area A_i, and $H(x)$ is the Heaviside step function, as

$$M_u \equiv \frac{\sum_i A_i \,\mathrm{div}_i\, H(-\mathrm{div}_i)}{\sum_i A_i} \qquad M_d \equiv \frac{\sum_i A_i \,\mathrm{div}_i\, H(\mathrm{div}_i)}{\sum_i A_i}$$

M_u and M_d are typically nonzero due to convective boundary layer circulations even when there is no precipitating convection (Figure 4). Therefore, we also define M_u^+, the mesonet surface divergence averaged over regions of convergence > 10^{-4} s^{-1}, and M_d^+, the mesonet surface divergence averaged over regions of divergence > 10^{-4} s^{-1} (Figure 5).

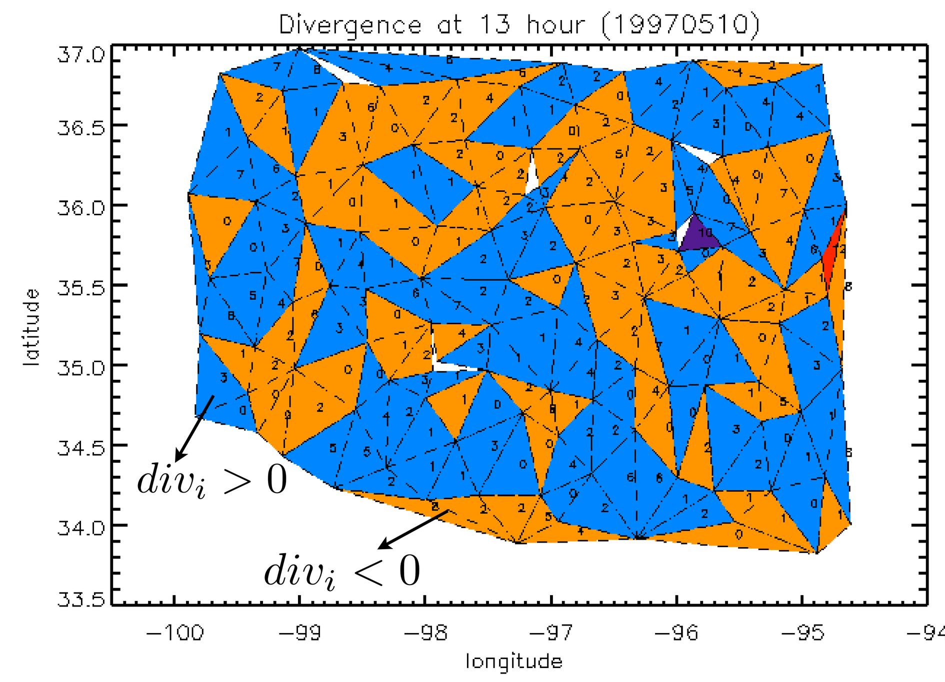

Figure 4. Divergence with colored triangles (values are shown in units of 10^{-5} s^{-1}) at 13 UTC on May 10, 1997

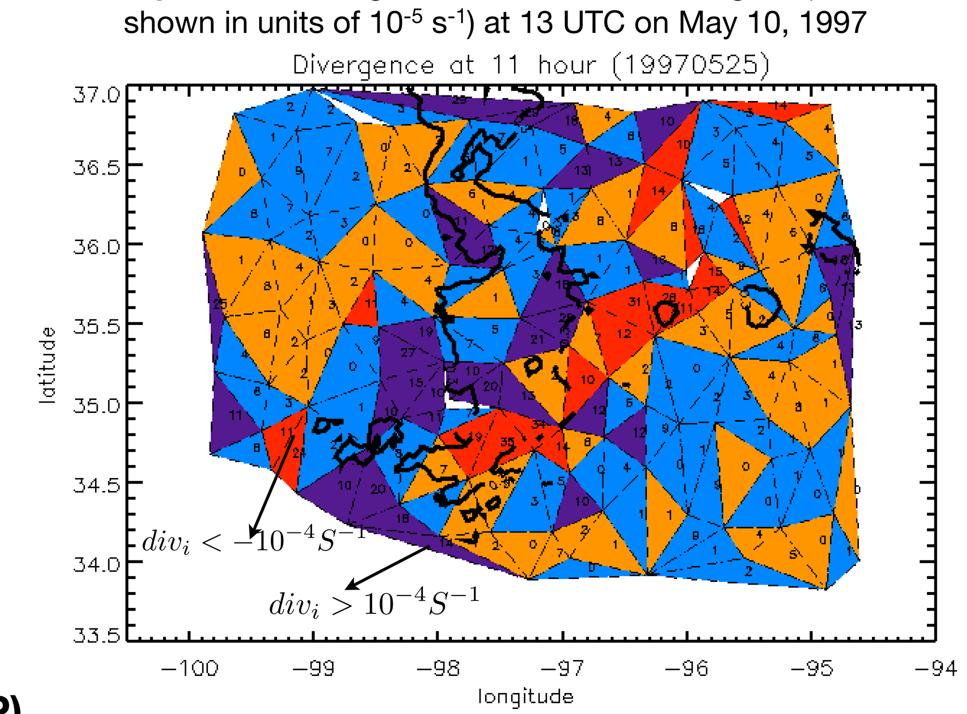

Figure 5. Divergence with colored triangles (values are shown in units of 10^{-5} s^{-1}) overlaid with precipitation rate contour (2 mm hr^{-1}) at 11 UTC on May 25, 1997

Lagged Correlations of Pcp Rate (P) and M_u, M_d, MSE s.d., and Wind Speed s.d.

Figure 6 shows that (1) M_d, M_u, M_u^+, and M_d^+ are correlated with P, (2) M_u^+ and M_d^+ are better correlated with P than are M_u and M_d, and (3) M_d and M_d^+ lag P and M_u and M_u^+ by about 1 h. These features suggest that it is possible to retrieve cloud–base mass fluxes from surface divergence and other properties.

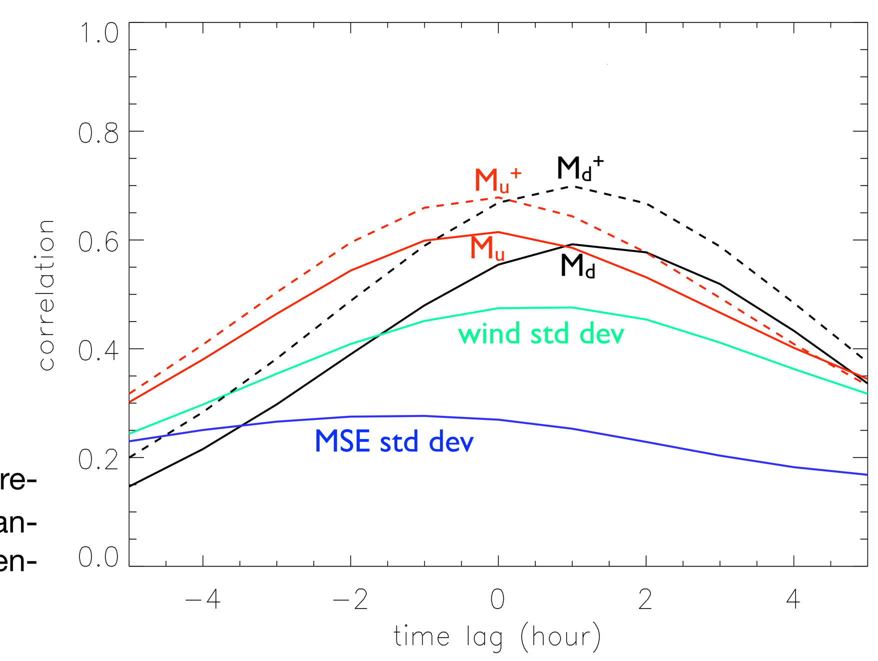

Figure 6. Lagged correlations of gridded hourly precipitation rate (P) and M_u, M_d, M_u^+, M_d^+, and standard deviations of wind speed and moist static energy (MSE) for May-August 1997

Evaluation of the 'Retrieval' Method Using Model Simulation Data

3D KWAJEX CRM Simulation

The 3D simulation was performed with the UU LES with a horizontal grid size of 1 km and a horizontal domain size of 128 km by 128 km. Both cloud updraft ($M_{c,u}$) and downdraft ($M_{c,d}$) mass fluxes are calculated at 1050 m. Two different methods are used to calculate div_i for each 32-km square. In the first method, u and v at all the points on the boundary of the 32-km square are used to calculate the true value of div_i for the square. In the second method, only u and v at the four corners of the 32-km square (representing mesonet stations) are used to estimate div_i. M_u and M_d calculated using the first method are called true M_u and M_d ($M_{u\ true}$ and $M_{d\ true}$). M_u and M_d calculated by using the second method are called meso M_u and M_d ($M_{u\ meso}$ and $M_{d\ meso}$).

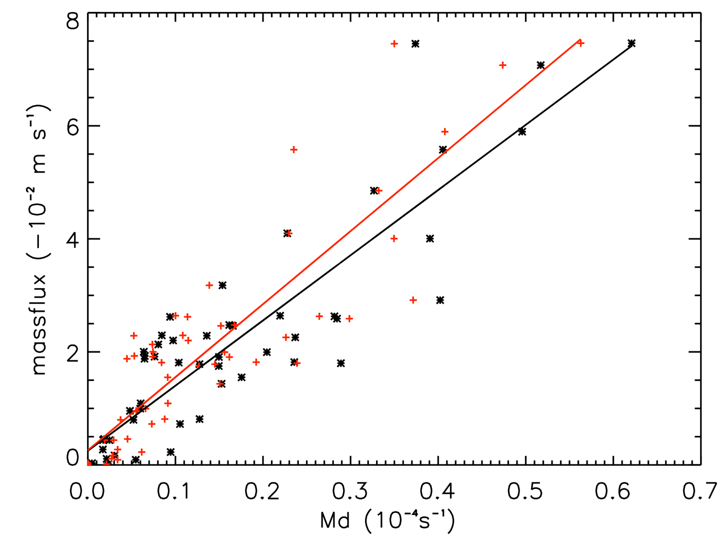

Figure 7. $M_{c,d}$ (m s^{-1}) versus $M_{d\ true}$ (black stars) and $M_{d\ meso}$ (red crosses). Black lines are line fits of $M_{c,d}$ and $M_{d\ true}$ and $M_{d\ meso}$. The correlations of $M_{c,d}$ and $M_{d\ true}$ and $M_{d\ meso}$ are 0.90 and 0.89.

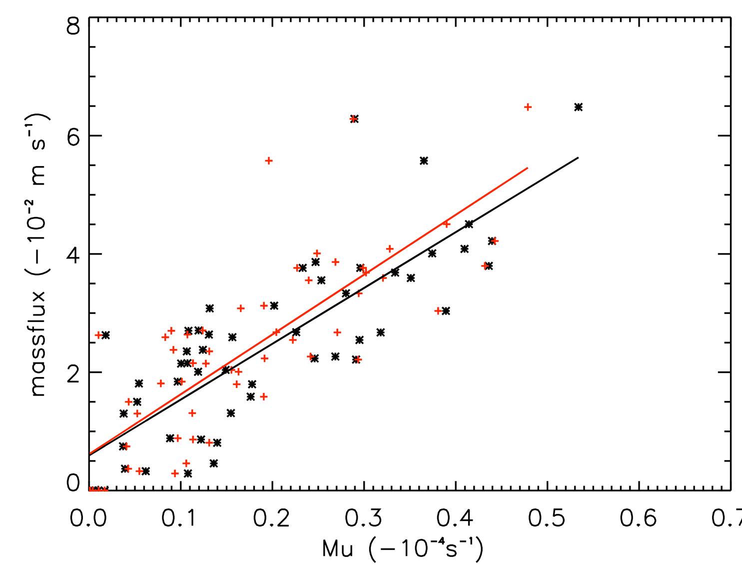

Figure 8. $M_{c,u}$ (m s^{-1}) versus $M_{u\ true}$ (black stars) and $M_{u\ meso}$ (red crosses). Black lines are line fits of $M_{c,u}$ and $M_{u\ true}$ and $M_{u\ meso}$. The correlations of $M_{c,u}$ and $M_{u\ true}$ and $M_{u\ meso}$ are 0.82 and 0.79.

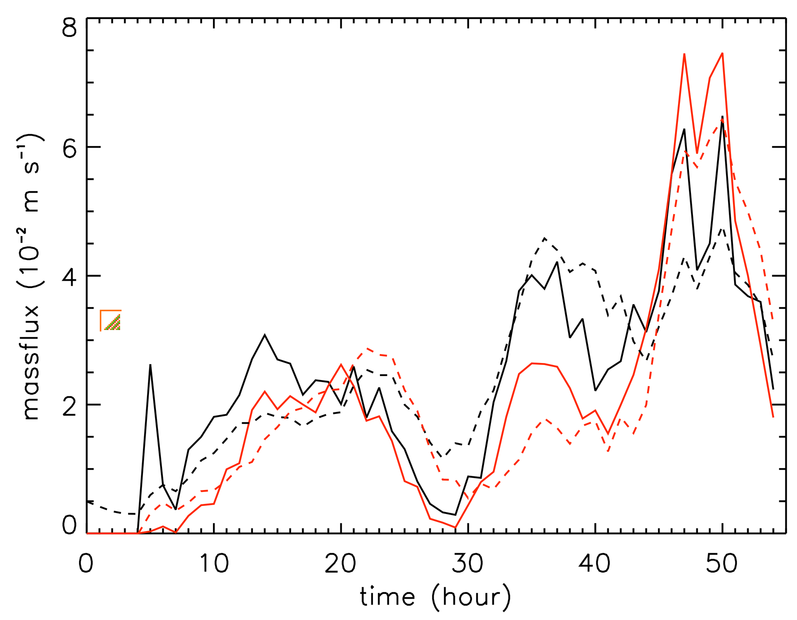

Figure 9. Time series of $M_{c,u}$ (black solid line) and $M_{c,d}$ (red solid line) at 1050 m AGL and $M_{c,u}$ estimated using $M_{u\ meso}$ (black dashed line) and $M_{c,d}$ estimated using $M_{d\ meso}$ (red dashed line).

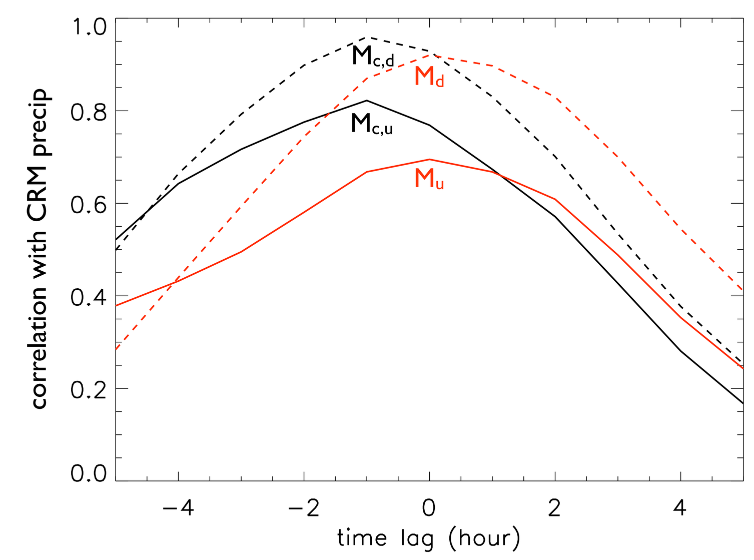

Figure 10. Lagged correlations of P with $M_{c,u}$, $M_{c,d}$, M_u, and M_d for the KWAJEX simulation.

Conclusions:

Both Oklahoma Mesonet observational data and results of two CRM simulations suggest that it is possible to estimate cloud-base mass fluxes from surface divergence field. The RMS errors of estimated $M_{c,u}$ and $M_{c,d}$ are 0.0097 m s^{-1} and 0.0086 m s^{-1} in the KWAJEX CRM simulation, and 0.0195 m s^{-1} and 0.0197 m s^{-1} in the 2D ARM case 3 simulation.

The observational data show that the maximum correlation of M_u and precipitation occurs about 0.5 h before the precipitation peak while the maximum correlation of M_d and precipitation occurs about an hour after the precipitation peak. The correlations of precipitation with M_u^+ and M_d^+ are larger than those with M_u and M_d.

The maximum correlations between P and M_u and M_d occurred at zero lag in KWAJEX. In ARM case 3 simulation, the maximum correlations between $M_{c,u}$ and $M_{c,d}$ with M_d, M_d^+, M_u, and M_u^+ occurred about an hour after the peak cloud mass fluxes. Surface divergence (convergence) correlates slightly better with $M_{c,d}$ than with $M_{c,u}$.

Acknowledgement: This research was supported by the National Science Foundation Science and Technology Center for Multi-Scale Modeling of Atmospheric Processes, managed by Colorado State University under cooperative agreement No. ATM-0425247.

References

Xu, K.-M., and Coauthors, 2002: An intercomparison of cloud-resolving models with the ARM summer 1997 IOP data. *Quart. J. Roy. Meteor. Soc.*, **128**, 593-624.

2D ARM Case 3 CRM Simulation

The 2D ARM case 3 simulation was performed by Xu et al. (2002). The cloud mass fluxes are calculated at 3 km AGL.

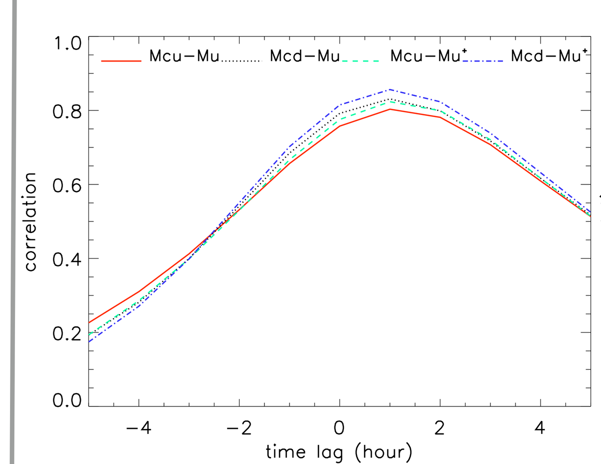

Figure 11. Correlations of $M_{c,u}$ with M_u, $M_{c,d}$ with M_u, $M_{c,u}$ with M_u^+ and $M_{c,d}$ with M_u^+.

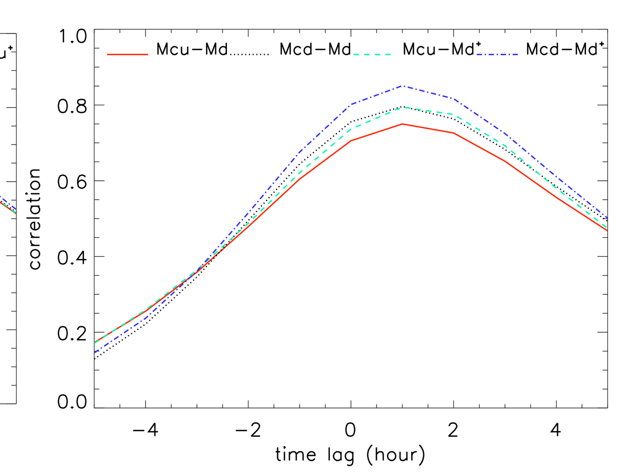

Figure 12. Correlations of $M_{c,u}$ with M_d, $M_{c,d}$ with M_d, $M_{c,u}$ with M_d^+ and $M_{c,d}$ with M_d^+.

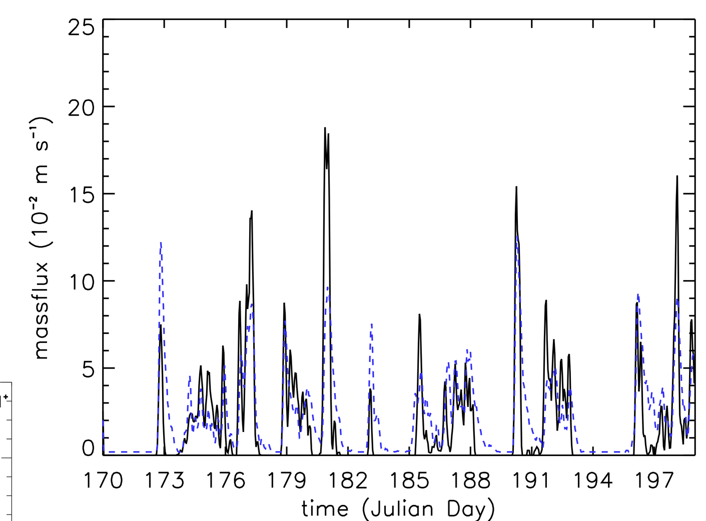

Figure 13. Time series of $M_{c,u}$ (black solid) at 3020 m AGL and its estimate using M_u^+ (blue dashed)

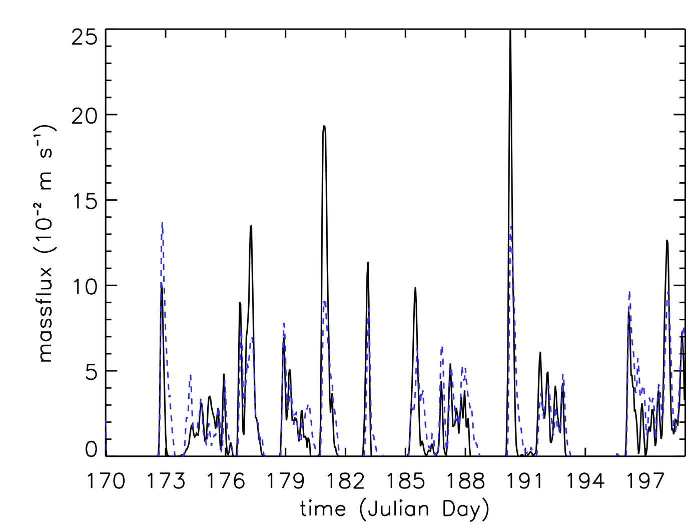

Figure 14. Time series of $M_{c,d}$ (black solid) at 3020 m AGL and its estimate using M_d^+ (blue dashed)